# A Modified Pilot-Aided Multi-Peak Search Frame Synchronization Algorithm for DVB-S2

Rodrigo A. R. Fischer, João Paulo Leite

***Abstract*— This work presents a modified version of an existing frame synchronization algorithm for DVB-S2 based satellite systems. The previous method uses pilot and header symbols to compute a decision metric, which is then fed to a peak search algorithm. The proposed method implements a more flexible decision metric and a peak search algorithm that allows for semi-analytical computations. This method is investigated through extensive computer simulations, which show that it is able to perform frame synchronization even at low signal-to-noise ratios and large carrier frequency offsets. Also, novel simulation results show a new perspective over the multi-peak search method.**

***Keywords*— DVB-S2, frame synchronization, pilot-aided algorithm, satellite communications.**

## I. Introduction

The DVB-S2 [1] standard adopts a framing structure composed of a header, the data fields and pilot symbols. The process of recovering the boundaries of the transmitted frames is called frame synchronization, which can be divided into two sub-processes: frame acquisition and frame tracking. These refer to, respectively, the process of identifying where the Start of Frame (SOF) is and the process where the receiver must be able to lock synchronization after the initial acquisition is complete. This initial acquisition step must be performed even with channel impairments such as frequency and phase offsets, since the impairment correction algorithms rely on the frame pilot structure, which is at a first moment not available. Usually, the modeling of the frame acquisition process and its analysis are considered separately from the frame tracking problem.

Many frame acquisition solutions have been published and most of them present a two-step algorithm, in which firstly a decision metric is computed and secondly the metrics are fed to a search algorithm that estimates the SOF position. In this sense, the work at [2] provides a procedure for ML estimation for a generic pilot-symbol-assisted transmission. Later at [3], modifications of this procedure resulted in a few detection metrics with various degrees of robustness regarding frequency offset. The work at [4] specialized the work of [3] to the DVB-S2X framing structure. However, the proposed search algorithm at [4] relies on the decoding of the Physical Layer Signaling Code (PLSC), which is not done reliably under the influence of unknown frequency offset. Some lower-complexity alternatives to the Choi-Lee Detectors (CLD) with satisfactory performance are represented by Post Detection Integration (PDI) detectors [5], [6], [7], [8].

When considering search algorithms, many options are available, such as threshold detection and argmax detection [2]. The greatest disadvantage of threshold detectors is that the optimum threshold setting that balances false and true acquisition probabilities is very sensitive to the operating Signal-to-Noise Ratio (SNR). On the other hand, the argmax proposed at [2] always selects a SOF after a fixed time, which results in a lock attempt even in the absence of a modulated signal. In this context, the multi-peak search [9] stands out as a trade-off between detector complexity and robustness. This method allows the detection of frames with unknown size at high frequency offset. The method at [9] was enhanced into the pilot-aided multi-peak search algorithm at [10].

The objective of this work is to present a complete description of a modified version of the frame acquisition method at [10]. In this sense, the Receiver Operating Characteristic (ROC) curve is obtained for a good range of relevant parameters. Also, by making some clever choices, the proposed algorithm allows a simple, yet well defined, semi-analytical framework to be used to derive meaningful insights on the technique. It is shown that if a complete analysis is not made wrong conclusions may arise from partial results.

This work is divided as follows: Section II presents an introduction to the the frame synchronization modeling and to the original and modified multi-peak search algorithms. Section III contains a performance analysis of the proposed algorithm based on simulation results. Finally, Section IV presents the conclusions.

## II. Frame Synchronization

### A. Reception Modeling

The adopted complex baseband received signal model corrupted by noise and with channel induced frequency offset is given by [11]

$$r_k = s_k e^{j(2\pi k \Delta f + \phi_0)} + n_k, \tag{1}$$

where $r_k$ represents the $k$-th sample at the matched filter output and $s_k$ represents the $k$-th transmitted complex symbol. The term $\phi_0$ is the phase offset, and the term $\Delta f = f_0 T_s$ is the normalized frequency offset, where $T_s$ is the symbol time and $f_0$ is the frequency offset. The additive noise is represented by $n_k$, a sample from a zero-mean complex white Gaussian noise distribution with a variance of $N_0/2$ per dimension.

This signal model is used in [3] to derive several decision metrics that are in several degrees less sensitive to frequency

Rodrigo A. R. Fischer, Electrical Engineering Department, University of Brasília, Brasília, Brazil, e-mail: rodrigoarfischer@gmail.com; João Paulo Leite, Electrical Engineering Department, University of Brasília, Brasília, Brazil, e-mail: jpauloleite@unb.br.

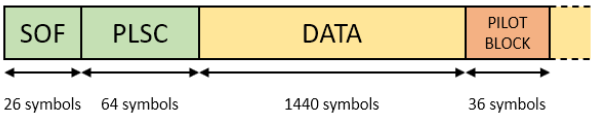


Fig. 1. DVB-S2 frame structure.

offset errors. Given a candidate symbol index $\mu$ for the start of frame and a set $K = \{s_0, \ldots, s_{L-1}\}$ of known symbols, the metric $L_3$ in [3] given by

$$L_3(\mu) = \left| \sum_{k=0}^{L-2} r_{\mu+k} r^*_{\mu+k+1} (s_k s^*_{k+1})^* \right|, \quad (2)$$

$(\cdot)^*$ denoting complex conjugation. The expression in Eq. (2) is also referred to as differential correlation. This metric is shown not to be susceptible to frequency offset errors [3]. Therefore, we define the received symbol differential at position $k$ as

$$r_k r^*_{k+1} \quad (3)$$

and the known symbol differential at position $k$ as

$$s_k s^*_{k+1}. \quad (4)$$

### B. Modified Pilot-Aided Multi-Peak Search

Figure 1 presents the DVB-S2 frame structure. The header is composed of a fixed 26-symbol field called Start of Frame (SOF) and a 64-symbol field called Physical Layer Signaling Code (PLSC), which are modulated using $\pi/2$-BPSK. All the symbols in the data and pilot field are scrambled by a pseudo-random sequence [1]. When pilot transmission is enabled, pilot blocks (PBs) containing 36 pilot symbols are distributed every 1440 data symbols. The synchronization process can be carried with or without the presence of PBs, as will be presented latter.

The authors of [10] have proposed a two-step frame synchronization algorithm. The first step consists of computing a decision metric for each possible position $\mu$ for the start of frame. Then, a search algorithm detects, based on the buffered metrics, a possible sample position for candidate as the start of frame. In this work, our approach differs from the one in [10] in two aspects. Firstly, the decision metric adopted considers also that pilot-less frames may be transmitted. Secondly, the peak search algorithm is modified by dividing it into acquisition rounds that are statistically independent and by increasing the number of attempts for some frame size configurations.

*1) Decision Metric:* The adopted decision metric $\Lambda(\mu)$ is defined as

$$\Lambda(\mu) = \max(|\Lambda_{SOF}(\mu) + \Lambda_{PLSC}(\mu) + \Lambda_{PIL}(\mu)|, \\ |\Lambda_{SOF}(\mu) - \Lambda_{PLSC}(\mu) + \Lambda_{PIL}(\mu)|), \quad (5)$$

where $\Lambda_{SOF}(\mu)$, $\Lambda_{PLSC}(\mu)$ and $\Lambda_{PIL}(\mu)$ are defined as in

$$\Lambda_{SOF}(\mu) = \sum_{i=0}^{24} r_{\mu+i} r^*_{\mu+i+1} {C^i_{SOF}}^*$$

$$\Lambda_{PLSC}(\mu) = \sum_{i=13}^{44} r_{\mu+2i} r^*_{\mu+2i+1} {C^i_{PLSC}}^*$$

$$\Lambda_{PIL}(\mu) = \sum_{k=1}^{N_{pil}} \sum_{i=0}^{34} r_{f(\mu,i,k)} r^*_{f(\mu,i,k)+1} {C^{i,k}_{PIL}}^*, \quad (6)$$

with

$$f(\mu, i, k) = 54 + \mu + i + 1476k. \quad (7)$$

On Eq. (6), $f(\mu, i, k)$ gives the received symbol index corresponding to a pilot symbol at position $i$ of the $k$-th pilot block of a frame starting at $\mu$. The terms $C^i_{SOF}$ and $C^i_{PLSC}$ represent, respectively, the known SOF and PLSC pilot symbols differentials, and $C^{i,k}_{PIL}$ represents the $i$-th known symbol differential from the $k$-th pilot block.

Since the pilot symbols are scrambled, the known differentials must take into account the symbol scrambling sequence. Even though the PLSC is unknown, it contains identical or negated bit repetition, depending on the pilot signaling bit [1]. Therefore, the PLSC differentials are known at even indexes, as seen in Eq. (6), and they can assume two sets of values, depending on the pilot signaling bit [4].

The approach at [10] considers only the transmission with pilots, and only this case is considered on their proposed decision metric. The present work considers also that frame formats without pilot symbols can be transmitted, so that the maximum of the two possibilities must be taken [9], [4]. The term $\Lambda_{PIL}$ can be set to zero when it is known that no pilots are present on the transmission and when a simplified version of the algorithm that only uses the header information is to be used, as in [9].

*2) Modified Peak Search Algorithm:* On the frame acquisition stage, the metric values are stored on a buffer with a size of two times the size of the largest possible frame, as shown on Figure 2. Then, for each possible frame size configuration, the buffer is divided into windows, on which the position of the largest metric values are stored, represented as arrows on Figure 2. The number of values stored for each window is the number of peaks analyzed [9]. If at two consecutive windows the pairwise distance between two values stored match the frame size, synchronization on that frame configuration is declared. If the whole buffer is tested without any locks, the whole process is reset and a new acquisition round is started. Since the buffer size is always larger than any possible frame and the buffer is reset on each round, consecutive acquisition rounds are statistically independent. The number of symbols consumed on each round is two times the number of symbols on the biggest frame size considered, and the amount of frames consumed on each round depends on the transmitted frame configuration.

## III. Computational Analysis

This work lays emphasis on the simulation analysis of the largest frame size configuration for the DVB-S2 standard:

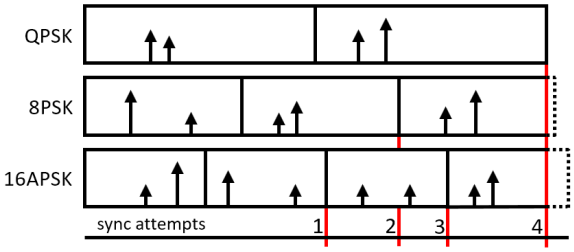


Fig. 2. Modified multi-peak detection scheme.

pilot-aided QPSK-modulated normal frame with a total of 33282 symbols including pilot and header symbols. This choice is justified by three main arguments. Firstly, the first acquisition attempt for this frame size configuration is the one preceded by the greatest amount of other synchronization attempts, as can be seen on Figure II. Therefore, this frame configuration is the most susceptible to false acquisitions on smaller frame size configurations. Secondly, the $\pi/2$-BPSK header and the PBs are more correlated to the QPSK data field than the other possible constellations for data transmission, since they contain exactly the same constellation points as the QPSK data field. Thirdly, when acquisition time is of concern, the largest frame size configuration yields the largest acquisition time.

Next, the acquisition process is modeled using a Markov chain and later simulation results are considered.

### A. Markov Chain Modeling of the Acquisition Stage

The fact that the acquisition rounds are independent allows the acquisition process to be modeled by a Markov chain, as depicted on Figure 3. This chain is composed of three states: a waiting state $W$ and two other absorbing states, namely acquisition $A$ and false detection $F$ states. With a Probability of Missed Acquisition (PMA) $p_M$ the machine misses frame acquisition and at the end of the round remains at state $W$. With Probability of True Acquisition (PTA) $p_{TA}$ the first attempt to declare synchronization occurs at the correct frame size configuration and at the correct SOF position. With Probability of False Acquisition (PFA) $p_{FA}$ the first attempt to declare synchronization occurs at the false frame size configuration or at the wrong SOF position, but at the correct frame size.

Since it is assumed that the largest frame size configuration is being transmitted, the transitions $W \to W$ and $W \to A$ occur at the end of the round after an elapsed time corresponding to two transmitted frames. The exact moment of a false acquisition can vary and the $W \to F$ transition time is unknown. However, in order to obtain rough estimates for the acquisition time and to consider the worse penalty for false frame acquisition, it will be considered that the transition $W \to F$ occurs at the end of the round.

Further, we define $P_s^i$, $s \in \{A, F\}$, as the probability of being absorbed at $s$ given that the machine started at a state $i \in \{A, F, W\}$. The analytical expressions of $P_A^W$ and $P_F^W$

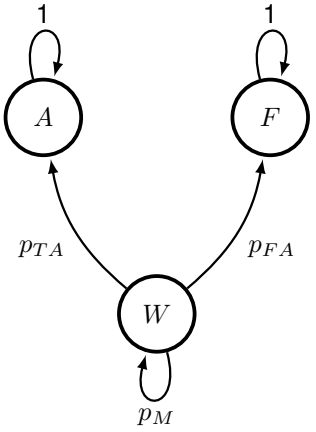


Fig. 3. Markov chain model for the frame acquisition stage.

TABLE I
SIMULATION CAMPAIGN CONFIGURATION

| | Modulation | Frame Size | Pilot | Total Size | $E_s/N_0$ | $\Delta_f$ |
|---|---|---|---|---|---|---|
| Campaign 1 | QPSK | Normal | Enabled | 33282 symbols | $-2.3$ dB | 0.2 |
| Campaign 2 | QPSK | Normal | Enabled | 33282 symbols | 0 dB | 0.2 |

are found to be

$$P_A^W = \frac{p_{TA}}{1 - p_M} \tag{8}$$

$$P_F^W = \frac{p_{FA}}{1 - p_M}, \tag{9}$$

where we note that, as expected, $P_A^W + P_F^W = 1$. We refer to $P_A^W$ as the Acquisition Probability. The Probability of True Acquisition in $N$ or less rounds, here denoted by $P_A(N)$, is

$$P_A(N) = \sum_{n=1}^{N} (p_M)^{n-1} \cdot p_{TA}. \tag{10}$$

Letting $N \to \infty$ on Eq. (10) provides the same result as obtained at Eq. (8), as expected.

The false detection state $F$ can also be modeled as a non-absorbing state with a penalty number of rounds of $N_p$, after which the false detection is detected by the frame tracking algorithm. Defining $N_A$ as the average number of rounds to reach $A$ given that the machine started at $W$, it can be shown that

$$N_A = \frac{1 + p_{FA} N_p}{p_{TA}}. \tag{11}$$

This expression confirms that as $p_{TA} \to 0$, $N_A \to \infty$ and that the greater $N_p$ or $p_{FA}$ are, the greater $N_A$ is.

### B. Simulation Results

In order to assess the performance of the proposed method, two campaigns were setup on a custom-made Python simulator as shown in Table I. However, the obtained results were not compared to previous results at [9], [10], since the authors don't completely define their algorithm testing conditions. Also, such previous results were not replicated in this work since this would require to use more well defined testing conditions and other assumptions about the algorithms, which could be characterized as a modification of the original methods.

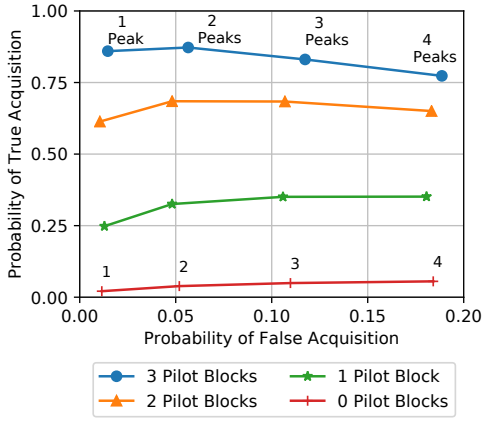


Fig. 4. Receiver Operating Characteristic (ROC) curve for Campaign 1 at $E_s/N_0 = -2.35$ dB.

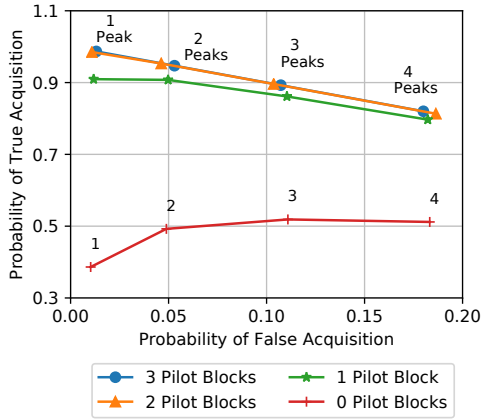


Fig. 5. Receiver Operating Characteristic (ROC) curve for Campaign 2 at $E_s/N_0 = 0$ dB.

All 12 possible frame sizes configurations were considered on the search algorithm for QPSK, 8PSK and 16APSK modulations.

Figures 4 and 5 show the Receiver Operating Characteristic (ROC) curves for Campaign 1 and 2 respectively, for multiple options for the number of PBs used on the decision metric. It can be seen that the points corresponding to a fixed number of PBs are approximately vertically aligned, meaning that increasing the number of PBs increases the probability of true acquisition without greater changes on the probability of false acquisition. Also, increasing the number of peaks always caused an increase on the PFA, since the greater the number of peaks the greater is the amount of tests performed on smaller window sizes.

On Figure 5 it can also be seen that the increase of the number of peaks causes a dramatic decrease on the PTA when 2 or 3 PBs are used. This is because in this scenario the PTA and PFA sum to almost one, leaving almost no chance for any missed detection. Then, increasing the number of synchronization attempts by increasing the number of peaks actually induces an increase in PFA, which causes the PTA to drop. When considering the scenario at Figure 4, even though the PFA always increase when increasing the number of peaks, the PMA is not close to zero, and increasing the number of peaks may actually result in converting a missed acquisition in a true acquisition.

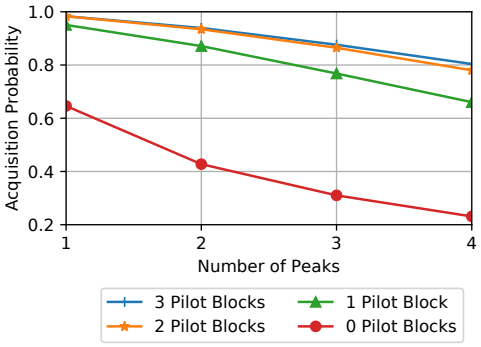


Fig. 6. Acquisition probabilities for Campaign 1 at $E_s/N_0 = -2.35$ dB.

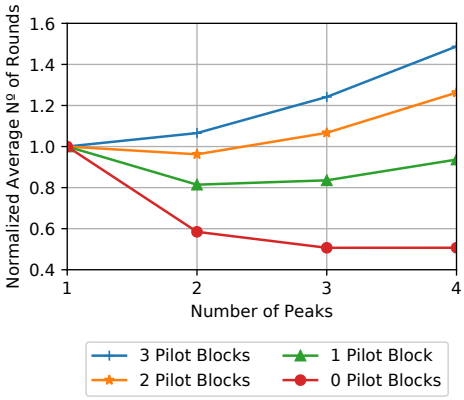


Fig. 7. Mean number of acquisition attempts $N_A$ for Campaign 1 at $E_s/N_0 = -2.35$ dB.

The expression on Eq. (8) was used to compute the acquisition probabilities for Campaign 1, which are shown in Figure 6. It can be seen that considering the impact of $p_M$ and $p_{FA}$ the absorption acquisition probabilities decrease as the number of peaks increase, even though Figure 4 shows an increase in PTA for some cases. In order to visualize the impact of $p_M$ and $p_{TA}$ on the average number of rounds to acquisition, Eq. (11) was used. Figure 7 shows the normalized average number of rounds, where normalization was done separately for each PB configuration. From this figure it can be seen that the average time for acquisition increases or decreases when increasing the number of peaks depending on the algorithm parameters. Therefore there is no rule of thumb when choosing how many peaks should be considered on the search. Simulations or experimental results on the receiver must be made for each configuration.

Table II summarize the best observed performance for both campaigns. It can be seen that at a time of 3 rounds, a total of 6 frames, the probability of true acquisition approaches the final acquisition probability.

## IV. Conclusion

This work presented a pilot-aided frame synchronization algorithm for the DVB-S2X standard. The proposed method differs significantly from the methods on [9], [10] on the search

TABLE II
NUMERICAL SIMULATION RESULTS

| Campaign | Peaks | Pilot Blocks Considered | PFA (%) | PTA (%) | PTA in 3 or Less Rounds (%) | Acquisition Probability (%) |
|---|---|---|---|---|---|---|
| 1 | 1 | 3 | 1.46 | 85.96 | 98.13 | 98.32 |
| 2 | 1 | 3 | 1.31 | 98.67 | 98.68 | 98.68 |

algorithm and differs slightly on the decision metric. The performance analysis at [9] considered only the probability of true acquisition in order to evaluate the performance impact of increasing the number of peaks. However, a more complete analysis using the proposed semi-analytical modeling shows that the true acquisition probability alone is not good enough metric do evaluate the expected acquisition time. The obtained results show that an undesired increase in acquisition time may occur when increasing the number of peaks.

The proposed method presents good performance even for a low signal-to-noise ratio of $-2.35$ dB and a normalized frequency offset of $20\%$, where synchronization was declared with a $98\%$ probability within 6 frames using 3 pilot blocks and one peak on the search algorithm.

## REFERENCES


[1] *Digital Video Broadcasting (DVB); Second generation framing structure, channel coding and modulation systems for Broadcasting, Interactive Services, News Gathering and other broadband satellite applications; Part 1: DVB-S2*, ETSI Standard EN 302 307-1, Nov. 2014.

[2] J. A. Gansman, M. P. Fitz and J. V. Krogmeier, "Optimum and suboptimum frame synchronization for pilot-symbol-assisted modulation," in IEEE Transactions on Communications, vol. 45, no. 10, pp. 1327-1337, Oct. 1997, doi: 10.1109/26.634696.

[3] Zae Yong Choi and Y. H. Lee, "Frame synchronization in the presence of frequency offset," in IEEE Transactions on Communications, vol. 50, no. 7, pp. 1062-1065, July 2002, doi: 10.1109/TCOMM.2002.800815.

[4] Sun, F.-W., Jiang, Y. and Lee, L.-N. (2004), Frame synchronization and pilot structure for second generation DVB via satellites. Int. J. Satell. Commun. Network., 22: 319-339. doi:10.1002/sat.793

[5] G. E. Corazza, P. Salmi, A. Vanelli-Coralli and M. Villanti, "Differential and non-coherent post detection integration techniques for the return link of satellite W-CDMA systems," The 13th IEEE International Symposium on Personal, Indoor and Mobile Radio Communications, Pavilhao Altantico, Lisboa, Portugal, 2002, pp. 300-304 vol.1, doi: 10.1109/PIMRC.2002.1046709.

[6] P. Kim, G. E. Corazza, R. Pedone, M. Villanti, D. Chang and D. Oh, "Enhanced Frame Synchronization for DVB-S2 System Under a Large of Frequency Offset," 2007 IEEE Wireless Communications and Networking Conference, Kowloon, 2007, pp. 1183-1187, doi: 10.1109/WCNC.2007.224.

[7] J. W. Park, M. H. Sumwoo, P. S. Kim and D. Chang, "Low complexity synchronizer architecture based on common autocorrelator for Digital Video Broadcasting system," 2009 16th International Conference on Digital Signal Processing, Santorini-Hellas, 2009, pp. 1-4, doi: 10.1109/ICDSP.2009.5201133.

[8] G. Albertazzi et al., "On the adaptive DVB-S2 physical layer: design and performance," in IEEE Wireless Communications, vol. 12, no. 6, pp. 62-68, Dec. 2005, doi: 10.1109/MWC.2005.1561946.

[9] Li Qing, Zeng Xiaoyang, Wu Chuan, Zhang Yulong, Deng Yunsong and J. Han, "Optimal frame synchronization for DVB-S2," 2008 IEEE International Symposium on Circuits and Systems, Seattle, WA, 2008, pp. 956-959, doi: 10.1109/ISCAS.2008.4541578.

[10] Yulong Zhang, Xubin Chen, Wenhua Fan, Jun Han and Xiaoyang Zeng, "Robust and reliable frame synchronization method for DVB-S2 system," 2010 Wireless Telecommunications Symposium (WTS), Tampa, FL, 2010, pp. 1-5, doi: 10.1109/WTS.2010.5479625.

[11] F. Ling, "An Overview of Digital Communication Systems," in *Synchronization in Digital Communication Systems,* 1st ed. Cambridge, United Kingdom: Cambride University Press, 2017, ch. 1, sec. 1.3.3.2, p. 17.